PARTICLE IMAGE VELOCIMETRY MEASUREMENTS ON A TURBULENT AIR JET OVER A FLAT PLATE

Ştefan-Mugur SIMIONESCU[1], Ümran DÜZEL[2], Claudia ESPOSITO[3], Zdeněk ILICH[4], Diana BROBOANĂ[5]

Particle Image Velocimetry is a non-intrusive laser optical measurement technique based on the velocity measurement of tracer particles carried by a fluid. PIV can be applied to virtually any kind of flow, as long as it is transparent to enable imaging of particles. The aim of this study is to become familiar with the technique and use its possibilities in turbulent flow characterisation. In the present case, the technique has been used in order to investigate the velocity field of a turbulent air flow over a flat plate at zero angle of attack, as well as the properties of the forming boundary layer.

Keywords: particle image velocimetry, boundary layer, turbulence, airflow.

1. Introduction

This article describes a study carried out by using the Particle Image Velocimetry (PIV) technique and presents its results. PIV is a laser optical measurement technique based on the measurement of the velocity of tracer particles carried by the fluid. It is capable to retrieve information about the velocity in a flow, providing a two-dimensional field measurement.

Two comprehensive reviews that constitute the basis of this study can be found in references [1] and [2]. The first one is a truly practical guide to the PIV technique, while the second one provides both a state-of-the-art of scientific research using PIV and some recent applications.

The basic principle of PIV is the following [1]: the instantaneous velocity of a fluid is measured through the determination of the displacement of tracer particles illuminated by the sheet of light. A CCD camera captures two successive images of the illuminated particles within a small time delay. Simply, once the elapsed time between the two images being taken is known, then the velocity can be obtained accordingly.

[1]PhD. Student, REOROM Laboratory, Hydraulics Department, University POLITEHNICA of Bucharest, Romania, e-mail: stefan_simionescu@yahoo.com
[2]Student, Von Karman Institute for Fluid Dynamics, Rhode Saint-Genèse, Belgium
[3]PhD. Student, Von Karman Institute for Fluid Dynamics, Rhode Saint-Genèse, Belgium
[4]PhD. Student, Von Karman Institute for Fluid Dynamics, Rhode Saint-Genèse, Belgium
[5]Ass. Prof., REOROM Laboratory, Hydraulics Department, University POLITEHNICA of Bucharest, Romania

PIV presents several advantages with respect to other techniques [1]. One is that, unlike other techniques like hot wire anemometry or pressure probes, PIV is a non-intrusive technique if the tracer particles are well chosen – for this, the Stokes number represents a good indicative [3]. Furthermore, PIV technique helps to measure a whole velocity field, instead of taking only punctual measurements. This allows the detection of spatial structures, even in unsteady flow fields.

The principle relies on tracer particles illuminated by a sheet of light. In the lightening process, pulsed laser units are generally used to produce the required amount of light. A light sheet is obtained from the beam using lenses, cylindrical and spherical. The laser and lenses alignment is very important to have effective imagining of particles. The sheet is settled to be parallel to the incoming flow. To visualize the flow in the light sheet, the fluid has to be seeded with particles. In order to follow the flow accurately, these particles need to be neutrally buoyant and small with respect to the flow. Concentration of the particles is also an important parameter and need to be chosen carefully. Very low concentration may lower limit the dimension of the interrogation window. Moreover, very high concentration may result in difficulties in cross-correlation map which has very high potential to high image noise. Camera settings are other parameters that have to be carefully set.

2. Boundary layer over a flat plate. Theoretical aspects

The boundary layer is the region of a flow close to a solid surface characterized by strong velocity gradients that will eventually give rise to turbulence. This phenomenon is of great importance in many engineering applications, including drag force control and heat transfer problems.

Considering the simple case of a flat plate immersed in a free stream of fluid with uniform velocity, we can state that when the fluid comes in contact with the solid fixed impermeable flat plate, its velocity is subjected to two boundary conditions: kinematic condition - no flow through the wall, and no slip condition - the tangential component of the flow velocity is zero at the wall.

The turbulent boundary layer can be divided into regions based on dimensionless wall distance y^+ [4], as shown in Figure 1. The inner boundary layer is the part of the turbulent boundary layer. The characteristic length and velocity for the turbulent boundary layer are the boundary layer thickness δ, defined as the normal distance from the wall at which the mean velocity in the boundary layer is 99% of U_∞, and respectively the free-stream velocity U_∞.

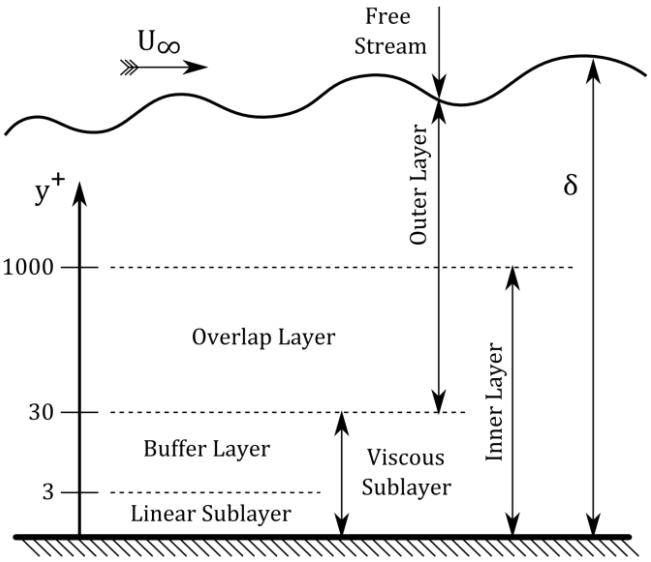

Fig. 1. Structure of turbulent boundary layer (adapted from [4])

In the flow over a flat plate, viscous effects are significant in a small layer close to the wall, namely the boundary layer. The properties of the boundary layer depend on the value of the *Reynolds number* Re; the boundary layer thickness δ can be expressed by the following empirical relation [5]:

$$\delta(x) = \frac{0.37 \cdot x}{Re_x^{\,1/5}} \tag{1}$$

The *Reynolds number* Re_L is calculated with the following formula:

$$Re_L = \frac{U_\infty \cdot L}{\nu} \tag{2}$$

where ν is the kinematic viscosity of the fluid in m^2/s.

A representation of the velocity profiles in the boundary layer is made using the nondimensional velocity U^+ and the nondimensional wall distance y^+ calculated as [5]:

$$U^+ = \frac{U}{U_\tau} \tag{3}$$

$$y^+ = \frac{y \cdot U_\tau}{\nu} \tag{4}$$

where U is the velocity measured, y the distance from the wall in m and U_τ is the friction velocity in m/s, computed as:

$$U_\tau = \sqrt{\frac{\tau_w}{\rho}} \tag{5}$$

The wall shear stress τ_w was computed with the formula expressed below [5], with C_f the skin friction coefficient:

$$\tau_w = \frac{1}{2}\rho {U_\infty}^2 C_f \tag{6}$$

3. Experimental setup

The tests have been performed in a low speed, open circuit wind tunnel. The experimental setup is presented in Figure 2. In the present study case two free stream velocities were considered: by measuring with an anemometer, the velocities for the tests were set to be $U_{\infty_1} = 5\ m/s$ and $U_{\infty_2} = 10\ m/s$. For a length L measured from the leading edge of the wind tunnel flat plate and ranging from $0.72\,m$ to $0.76\,m$, the computed values of Re_L go from 238000 to 251000 for U_{∞_1}, respectively from 480000 to 506500 for U_{∞_2}. The theoretical values of the boundary layer thickness $\delta(L)$ range from $22.39\,mm$ to $23.39\,mm$ for U_{∞_1} and from $19.46\,mm$ to $20{,}33\,mm$ for U_{∞_2}.

The test section size is 200 x 80 mm. A specific configuration of flow through the test section was studied, namely a flat plate at zero angle of attack, with 40 mm width. In the test section the surface of the plate is made of polished metal, "mirror", which reflects the laser light, without deteriorating the image quality, and offers a good control for the alignment of the laser sheet perpendicular to the plate and also increases the intensity of light in the test section. The tracer particles are seeded into the flow by using a smoke generator connected to the wind tunnel fan.

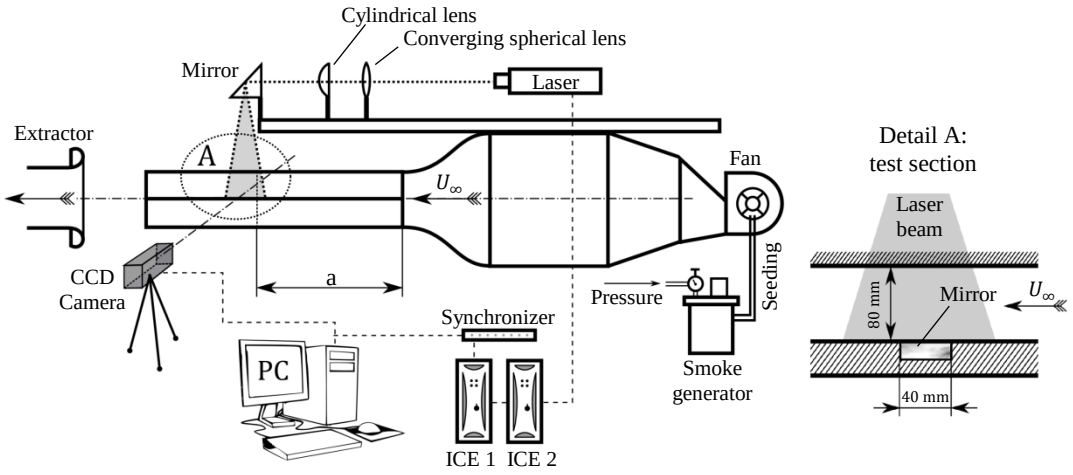

Fig. 2. Sketch of the PIV experimental setup with detail on the test section

The illumination of the particles is made by using a pulsed laser of type MiniYAG. Its technical data are: wavelength *532 nm*; maximum frequency *15 Hz*; energy *200 mJ*; starting diameter *6 mm*; pulse duration *8 ns*. An important parameter for the laser is its intensity, which can be changed by changing the Q-Switch time. The flush-lamp current is changing in time, and as consequence the pumping of the laser rod is changing as well and thus the different Q-Swich delays which are connected to the pulse time, will manifest themselves in different light intensities [6]. The laser system has two separate cavities, which follow each other within a very short time (separation time), before recharging.

Two lenses, one of cylindrical type and one spherical, are used, the first one to transform the laser beam into a sheet, and the second to collimate the sheet, which is then reflected to a perpendicular direction towards the wind tunnel test section, through a 45° standing mirror. The thickness of the laser sheet should be set as small as possible, by changing the relative position of the two lenses [7].

The camera used during the tests is a PCO Sensicam. It is able to capture two subsequent images (image pairs) with a separation time of 200...1000 ns, which are then recorded on the same picture. In order to be able to carry out a successful PIV measurement, laser and camera should be synchronized. This is performed using the Motion Pro Timing Hub synchronizer, which provides 8 independent synchronization signals, with 20 ns resolution [8].

4. Results

4.1. Velocity profiles and boundary layer thickness

The free stream velocity as computed from the PIV measurements is for the two cases respectively $U_{\infty_1} \cong 5.074\, m/s$ and $U_{\infty_2} \cong 10{,}23\ m/s$. The velocity profiles in the boundary layer are shown in Figure 3. The computed boundary layer thickness, as the distance from the wall at which the velocity is 99% of the free stream velocity, is $\delta_1 = 28.81\ mm$, respectively $\delta_2 = 25{,}52\ mm$.

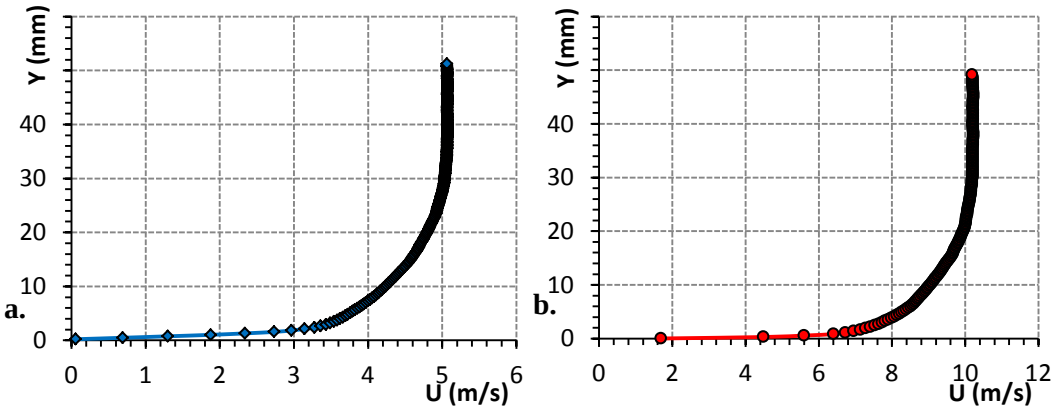

Fig. 3. Velocity profiles in the boundary layer: a) 5 m/s; b) 10 m/s

In Figure 4.a the velocity vector field map for the case $U_{\infty_1} = 5\ m/s$ is presented. The dimensionless velocity profile has been computed by nondimensionalizing the velocity U by the free stream velocity U_∞ and the wall distance y by the boundary layer thickness δ. A comparison between the dimensionless velocity profiles for the two studied cases is presented in Fig. 4.b.

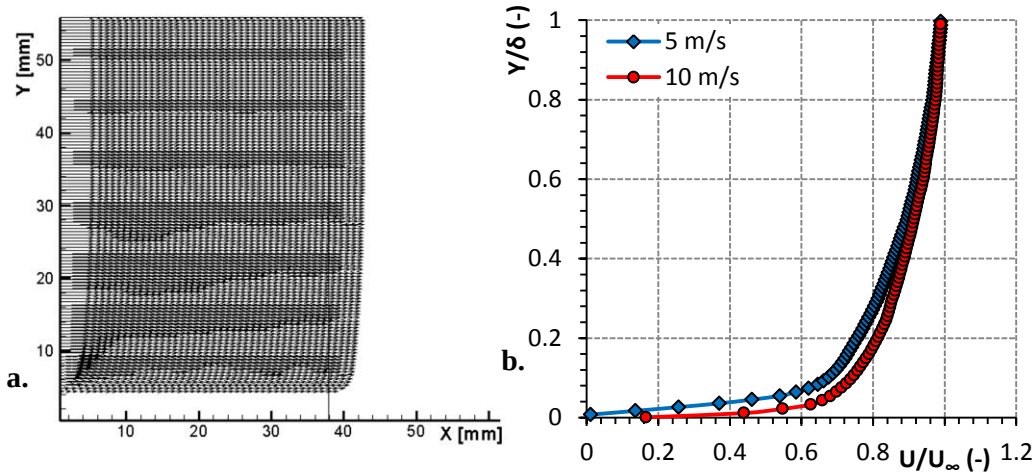

Fig. 4. Velocity vectors field map for $\boldsymbol{U_{\infty_1} = 5\ m/s}$ (a) and dimensionless velocity profiles (b)

The experimental results were compared to the theoretical reference values [5] (one seventh power law) in Figure 5. A good agreement was found, which confirm the accuracy of the PIV measurements.

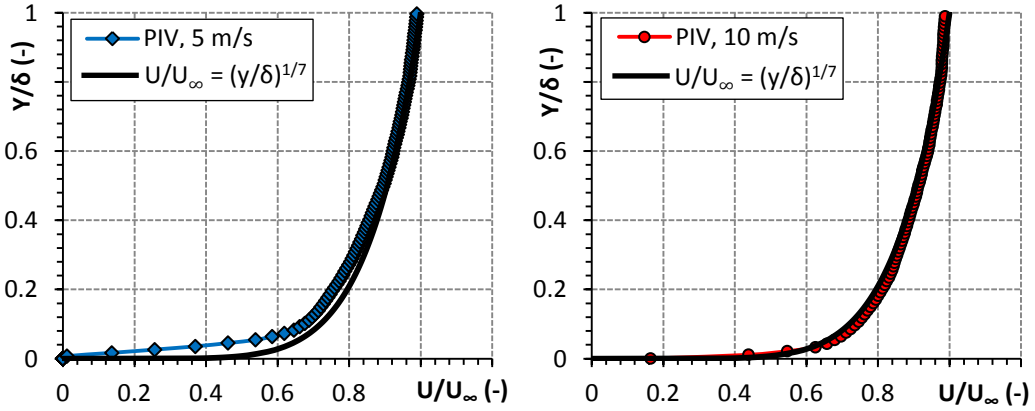

Fig. 5. Comparison of experimental results with the 1/7 power law

For a better sight of the different regions of the boundary layer, it is possible to plot the dimensionless velocity profile in a semilogarithmic scale. A graph with U^+ against y^+ was computed.

A comparison of the results from the PIV measurements with the universal velocity profile is performed, and the results are plotted in Figure 6. A global agreement of the experimental results compared to the theoretical reference can be noticed. Two aspects are noticed: for the lower flow velocity, in the whole viscous sublayer ($y^+ < 30$) a shift from the theoretical values is noticeable. As for the higher flow velocity, the first measurement point finds itself at $y^+ \cong 10$, so closer to the wall no experimental data was taken due to the higher gradients in the tangential velocity field.

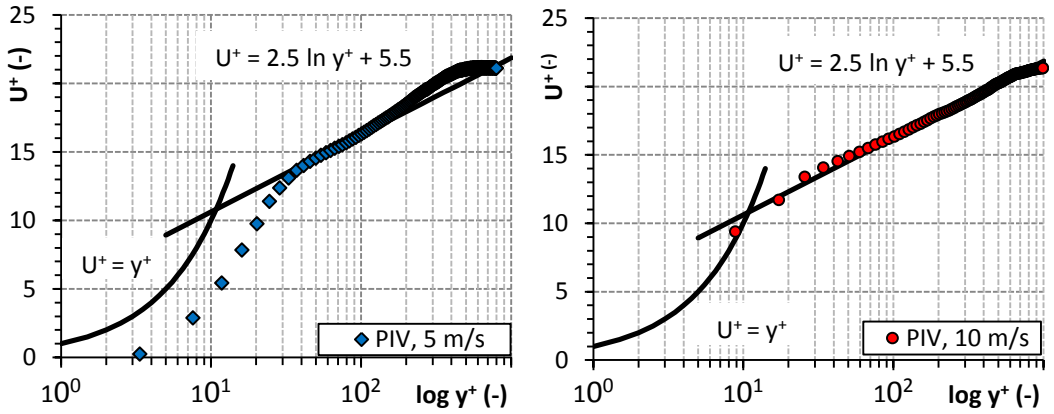

Fig. 6. Comparison between the universal profile and PIV results

4.2. Turbulence intensity profile. Skin friction coefficient

The local turbulence intensity field map can be seen in Figure 7. The maximum value of turbulence intensity is close to the wall: $TI_{max} = 0.32$ for the case with $5\ m/s$ free stream velocity, respectively $TI_{max} = 0.22$ for $10\ m/s$ free stream velocity.

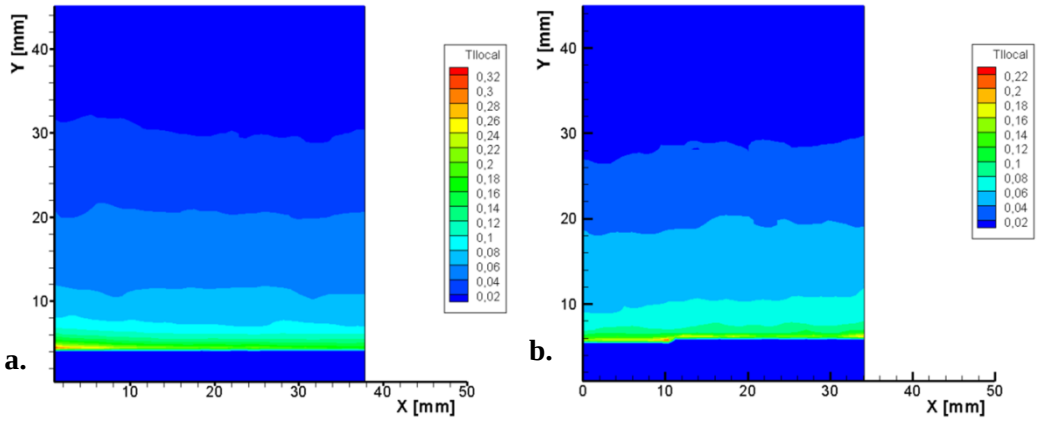

Fig. 7. Local turbulence intensity map: a. 5 m/s; b. 10 m/s

In Figure 8 the turbulence intensity profile in the boundary layer for the 2 studied cases is plotted.

In order to obtain wall scaling factors it is required to determine the friction velocity U_τ and friction coefficient C_f. Hence, Bradshaw's method is applied to obtain the skin friction coefficient [5]. The method is based on the plot of U/U_∞ with respect to $y \cdot U_\infty/\nu$ - see Figure 9.

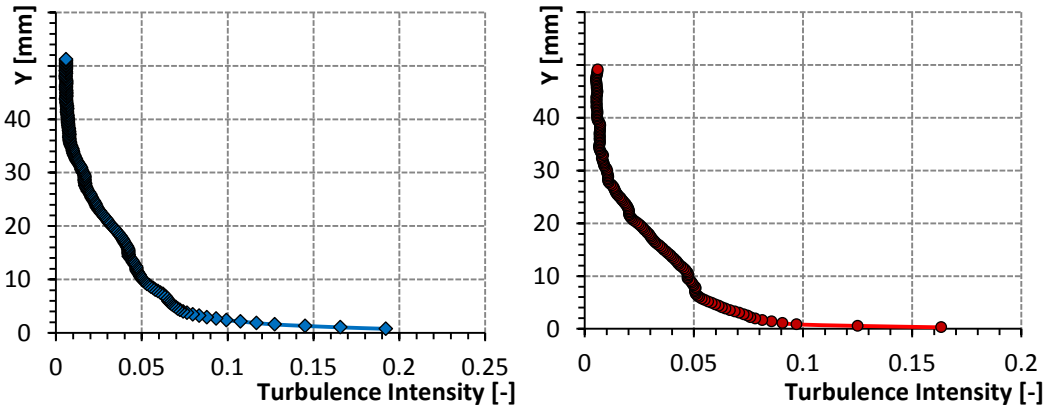

Fig. 8. Turbulence intensity profile in the boundary layer: a. 5 m/s; b. 10 m/s

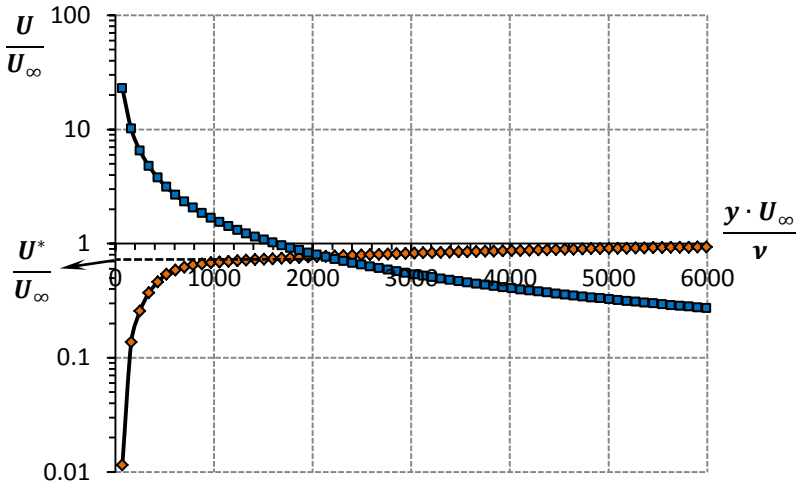

Fig. 9. Determining the $\boldsymbol{U^*}$ velocity with Bradshaw's method, for $\boldsymbol{U_{\infty_1} = 5\ m/s}$

Observing that the point at $y^+ = 100$ is clearly in the logarithmic layer and the corresponding value of $U^+ = 16.24$. It results that for the corresponding point:

$$\frac{U}{U_\infty} = \frac{1624 \cdot \nu}{y \cdot U_\infty} \tag{7}$$

Having plotted this relation on the same plot, it can be found that the point at which it intersects the experimental curve is the point at $y^+ = 100$. U^*/U_∞ is the velocity at this point, and the calculated value for U^* is $U^* = 3{,}90\ m/s$ for $U_\infty = 5\ m/s$ and $U^* = 7{,}78\ m/s$ for $U_\infty = 10\ m/s$. The skin friction coefficient can be determined as [5]:

$$C_f = 2 \cdot \left[\frac{1}{16.24}\left(\frac{U^*}{U_\infty}\right)\right]^2 \tag{8}$$

The computed values and a comparison with theoretical values from [9] are provided in Table 1.

Table 1

Skin friction coefficient C_f: comparison with theory

Free-stream velocity	PIV results	Theory
$5\ m/s$	0.00447	0.0043
$10\ m/s$	0.00438	0.0042

4.3. Integral parameters

The computation of several main integral parameters was performed, mainly for the quantitative evaluation of the experimental results. The values are plotted in Table 2. The skin friction coefficient C_f (and thus the corresponding shear stress τ_w and friction velocity U_τ) is determined using the Bradshaw method [5]. The boundary layer thickness δ corresponds to a velocity equals to 99% of U_∞.

Table 2

Integral parameters for the two velocities tested

Parameter	PIV 5 m/s	PIV 10 m/s
$\boldsymbol{U^*\ (m/s)}$	3.8974	7.7760
$\boldsymbol{C_f\ (-)}$	0.00447	0.00438
$\boldsymbol{\tau_w\ (Pa)}$	0.0684	0.2723
$\boldsymbol{u_\tau\ (m/s)}$	0.2399	0.4788
$\boldsymbol{\delta\ (mm)}$	28.81	25.52
$\boldsymbol{U_\infty\ (m/s)}$	5.0748	10.2316
$\boldsymbol{L_{min}\ (m)}$	0.72	0.72
$\boldsymbol{L_{max}\ (m)}$	0.76	0.76
$\boldsymbol{Re_{L\,min}\ (-)}$	238035	479919
$\boldsymbol{Re_{L\,max}\ (-)}$	251259	506581

5. Conclusions

Particle Image Velocimetry measurements have been carried out to investigate the velocity field in a wind tunnel. In particular, a specific configuration of flow has been considered: turbulent air flow over a flat plate.

A preliminary adjustment of the different relevant parameters has been performed in order to find optimal values and to understand their influence on the results quality: magnification factor, separation time, laser intensity, diaphragm aperture, seeding density.

The reference flow concerns the boundary layer over a flat plate for two different velocities. The dimensionless velocity profile was obtained for the free stream velocities of $5\,m/s$ and $10\,m/s$ and the comparison with the universal law of the boundary layer and $1/7^{th}$ power law was carried out. A good agreement between theory and experimental data from PIV measurements was noticed. The computing of the skin friction coefficient was performed by using the Bradshaw's method, and the PIV and theoretical values are very close. Finally, attention has been focused on the turbulence field, showing how it increases close to the wall.

Acknowledgement

The authors would like to acknowledge the support of the Von Karman Institute for Fluid Dynamics, Rhode Saint-Genèse, Belgium, where the experiments were performed.

The work has been funded by the Sectorial Operational Programme Human Resources Development 2007-2013 of the Ministry of European Funds through the Financial Agreement POSDRU/159/1.5/S/132395.

R E F E R E N C E S

[1]. *M. Raffael, C. E. Willert, S. T. Wereley, J. Kompenhaus,* Particle Image Velocimetry. A Practical Guide. Second edition. Springer, London, 2007;

[2]. *A. Schroder, C. E. Willert*, Particle Image Velocimetry. New Developments and Recent Applications. Topics in Applied Physics, **Vol. 112**, Springer, London, 2008;

[3]. *J. Anthoine, T. Arts, H. L. Boerrigter, J. M. Buchlin, M. Carbonaro, G. Degrez, R. Denos, D. Fletcher, D. Olivari, M. L. Riethmuller, R. A. van den Braembussche,* Measurement Techniques in Fluid Dynamics. An Introduction, Von Karman Institute for Fluid Dynamics, 3rd revised edition, 2009;

[4]. *Y. Kawaguchi, T. Segawa, et al.,* Experimental study on drag-reducing channel flow with surfactant additives – spatial structure of turbulence investigated by PIV system, International Journal of heat and fluid flow, **Vol. 23**, pp. 700-709, 2002;

[5]. *G. Degrez,* Two-dimensional boundary layers, Revised edition, Course note 143, Von Karman Institute for Fluid Dynamics, November 2013;

[6]. *Horvath Istvan Antal, Trianon Tagado,* PIV System Synchronisation at VKI, Von Karman Institute for Fluid Dynamics, 2010;

[7]. *AR / EA Faculty and PhD.*, Guidelines for Measurement Techniques Laboratories, VKI Course Notes 191, October 2013;

[8]. *F. Scarano, M. L. Riethmuller*, Iterative multigrid approach in PIV image processing with discrete window offset, Experiments in Fluids 26, 1999, Springler Verlag;

[9]. *** Boundary Layer DNS/LES Data, 11/23/2014, Retrieved from 'http://www.mech.kth.se/~pschlatt/DATA/#DNS'.